Sample Selection Algorithms for Enhanced MIMO Antenna Measurements Using Mode-Stirred Reverberation Chambers

Adoración Marín-Soler, Mathias Grudén, *Student Member, IEEE*, Juan D. Sánchez-Heredia, Paul Hallbjörner, Antonio M. Martínez-González, Anders Rydberg, *Member, IEEE*, and David A. Sánchez-Hernández, *Senior Member, IEEE*

***Abstract*—Mode-stirred reverberation chambers (MSRCs) are a useful tool for measuring several wireless-related MIMO antenna parameters. In a conventional single-cavity MSRC, the emulated fading environment is isotropic and the amplitude of the signal is Rayleigh distributed. Previous contributions have enhanced the emulation capabilities of MSRCs so as to include the ability to emulate Rician- and non-isotropic fading environments. In this contribution, arbitrary amplitude probability density functions (PDF) emulation using a MSRC is presented by selecting parts of the sample set that forms different statistical ensembles. Several algorithms are presented and compared in terms of computation time and power accuracy using simulated as well as measured data from different MSRCs to obtain Rician, on-body and amplitude PDFs of standardized models. The technique is patent-protected by EMITE.**

***Index Terms*—Algorithms, antenna measurements, fading channels, genetic algorithms.**

I. Introduction

A methodology to measure the MIMO performance of antenna sets using a mode-stirred reverberation chamber (MSRC) was selected by standardization bodies in 2008 [1]. An MRSC contains a set of mode stirrers that changes the boundary conditions of the main cavity of the chamber. The metal cavity, along with the stirrers, provides a multi-reflective environment which is repeatable and can be statistically studied. The repeatability and statistical nature of MSRCs make them a versatile tool for measuring a wide variety of MIMO antenna parameters [2]–[6].

Manuscript received August 23, 2011; manuscript revised December 03, 2011; accepted February 25, 2012. Date of publication May 23, 2012; date of current version July 31, 2012. This work was supported in part by the Spanish National R&D Programme through TEC2008-05811.

M. Grudén and A. Rydberg are with the Microwave and Terahertz Technology Group, Uppsala University SE-751 21 Uppsala, Sweden (e-mail: mathias.gruden@angstrom.uu.se; anders.rydberg@angstrom.uu.se).

J. D. Sánchez-Heredia, A. M. Martínez-González, and D. A. Sánchez-Hernández are with the Departamento de Tecnologías de la Información y Comunicaciones, Universidad Politécnica de Cartagena, Cartagena E-30202, Spain (e-mail: jd.sanchez@upct.es; toni.martinez@upct.es; david.sanchez@upct.es).

P. Hallbjörner is with the SP Technical Research Institute of Sweden, SE-501 15 Borås, Sweden (e-mail: paul.hallbjorner@sp.se).

A. Marín-Soler is with the EMITE, Edificio CEDIT, Parque Tecnologico Fuente Alamo, E-30320 Fuente Alamo, Murcia, Spain (e-mail: adoracion.marin@emite-ingenieria.es).

Color versions of one or more of the figures in this paper are available online at http://ieeexplore.ieee.org.

Digital Object Identifier 10.1109/TAP.2012.2201103

In its conventional design, an MSRC uses a single cavity. With perfect stirring, the real and imaginary parts of the rectangular components of the electric and magnetic field throughout the single-cavity become Gaussian distributed, independent with identical variances. Thus, the electric or magnetic field inside the single-cavity follows a Rayleigh probability density function (PDF) in amplitude and uniform distribution of phase, which resembles the multipath fading in urban scenarios of wireless communications systems. This initial design has been densely studied in the literature [7]–[12]. But in MSRCs, a term that was coined in 1995 [13], the fields do not necessarily have to be constrained to a single-cavity or even be provided in a reverberating mode to the researcher. In consequence, MSRCs may contain more than one metal cavity which could be coupled through a variety of means, including waveguides, slots or metal plates, among others. Likewise, the shape of these cavities does not have to be restricted to the canonical ones and additional software control and algorithms, along with stochastic handling of measured samples, allow extraordinary advantages to the engineer over conventional single-cavity reverberation chambers.

With the advent of 4G systems employing MIMO and the urgent need to employ fast, accurate and cost-effective MIMO Over-The-Air (OTA) test tools, the last few years have witnessed a large number of improvements in the emulating capabilities of MSRCs using non-conventional designs. Among the improvements that require hardware alterations we can mention the use of phantoms, absorbers, non-canonical shapes, multiple cavities or source stirring techniques to reproduce realistic distributions with diverse Power Delay Profiles (PDP), Root-Mean-Square Delay Spreads (RMS DS) or fading profiles such as keyholes, hyper-Rayleigh, Rician-fading, indoor environments, wideband in-vehicle environments, metallic windows, tree canopies, walls and other artefacts in buildings [14]–[22]. Among the improvements that use software alterations we can mention the recent ability to measure the radiation patterns of antennas using time-reversal techniques [23] or the extraordinarily innovative ability to measure angle-of-arrival using Fourier beamsteering [24].

These enhancements now make possible to evaluate, under different environments, novel antenna-associated parameters related to MIMO performance, such as correlation, diversity gain or capacity, among others, which were previously channel-only related issues. This has certainly made small, fast

and relatively-cheap MSRC's capabilities approach those of large, slow and expensive anechoic chambers, and has called the attention of the Antenna and Propagation community [2], [3], [14], [15], [17]–[20], [22], [23], [25], [26], [28]. This is because a large number of technical add-ons (quiet zone, RF probes, antennas, cables, phase shifters, etc.) with a large associated cost is needed to make anechoic chambers-based MIMO OTA tests effectively. A summary of recent advances in MSRCs can be found in [26].

Among these recent enhancements, the authors have recently presented a novel technique to emulate different amplitude PDF of fading distributions by sample selection [27]. By keeping or discarding samples from a large measured sample set it is possible to achieve a new arbitrary amplitude PDF which only consists of unmodified measured samples. The short contribution in [27] was limited to one MSRC, the use of Rayeigh-fading initial data and only Rician-fading target PDFs. In this paper several algorithms for the sample selection technique presented in [27] are analysed and compared with the use of both simulated and measured data, for two different MSRCs and targeting Rician-, on-body and standardized fading models amplitude PDFs. The analyses are performed in respect of distribution accuracy and computational time in an attempt to approach quasi-real-time operation of the new technique. Although the sample selection technique presented here cannot yet fully emulate all the physical parameters that characterise a fading environment through standardized models, such as angle of arrival (AoA), Power Angular Spectrum (PAS) or PDP, the new capabilities are certainly a step forward towards a potential emulation of arbitrary fading profiles using advanced MSRCs. This is extremely important as amplitude-only SCME models using diverse delay taps have been suggested at standardization bodies for initial tier 1 compliance testing stages, while advanced channel models are only to be employed in tier 2 testing [28]. In fact, the Rayleigh-fading channel emulated by anechoic-based MIMO OTA systems is an amplitude-only PDF [29].

II. Sample Selection Algorithms

The presented algorithms are based on the PDFs of the data. In a rich multipath environment, the real and imaginary parts of the complex amplitude of the received signal are Gaussian distributed around zero. In this environment the PDF of the amplitude can be described by the Rayleigh model

$$f_{Rayleigh}\left(|S_{21}|\right) = \frac{|S_{21}|}{s^2}\exp\left(-\frac{|S_{21}|^2}{2s^2}\right) \tag{1}$$

where $2s^2$ is the mean power of the signal. In a multipath environment with dominant line-of-sight (LoS) component the amplitude of the received signal becomes Rician distributed, with the PDF

$$f_{Ricean}\left(|S_{21}|\right) = \frac{|S_{21}|}{s^2}\exp\left(-\frac{|S_{21}|^2 + a^2}{2s^2}\right) I_0\left(\frac{|S_{21}|\,a}{s^2}\right) \tag{2}$$

where $I_0(\cdot)$ is the zero-order modified Bessel function of the first kind, a^2 is the power of the constant offset of the distribution (LoS component), and $2s^2$ is the power of the scattered part of the signal (non-LoS (NLoS) component). The Rician distribution is characterized by the K-factor, defined as the ratio between the direct and scattered powers by [20]

$$K = \frac{|\langle S_{21}\rangle|^2}{\left\langle |S_{21} - \langle S_{21}\rangle|^2 \right\rangle} = \frac{a^2}{2s^2}. \tag{3}$$

The K factor theoretically ranges from zero to infinite. Several references, however, describe practical K-factors from zero to a maximum of about 180 [30], [31]. All selected algorithms will select a subset of samples (final) from a large sample set (initial) that conform to a pre-defined statistical ensemble (target).

A. The Single Step Algorithm

In the first algorithm we define a relationship between the initial distribution and its target distribution counterpart by

$$f_{initial}(S_{21}) \cdot D(S_{21}) = f_{target}(S_{21}) \tag{4}$$

where $f_{initial}(S_{21})$ is the initial PDF, $D(S_{21})$ is a weighting function and $f_{target}(S_{21})$ is the target PDF [32]. The weighting function D is

$$D(S_{21}) = \frac{D_1(S_{21})}{\max(D_1(S_{21}))} \tag{5}$$

in which the amplitude is normalized to have a value between zero and unity. In this algorithm, the i_{th} measured sample with an amplitude of S_{21}^i, will be kept in the final subset only if $D(S_{21}^i) > U(0,1)$ is true, and it is discarded otherwise. The notation U(0,1) defines a random variable with uniform distribution between 0 and 1. Therefore, the function $D(S_{21})$ in the algorithm is used as a decision threshold for each sample such that it provides the probability of keeping the sample. The fact that a decision is taken once, without any iteration, is the reason why this algorithm was named the single step algorithm.

B. The Iterative Genetic Algorithm

In an attempt to get a better decision tool, an evolutionary method of a genetic algorithm (GA) [33] is also employed to optimize the fitness between the PDF of an ensemble of samples and the target PDF. The application of GA to the sample selection problem consists of assigning one binary variable (0 or 1) to each sample, denoting whether the sample will be in the final subset or not. The algorithm can be further constrained with a pre-defined minimum number of samples that we want in the final solution ensemble so as to conform to a set of goodness-of-fit tests. The employed error (fitness) function is a sum squared error (SSE) based function. Since for the sample selection problem we are looking for best fits to target PDFs, which range from 0 to 1, the conventional SSE formula was modified as

$$\varepsilon_{SSE} = \frac{\sum_{i=1}^{n}\left[f_{final}(i) - f_{target}(i)\right]^2}{\sum_{i=1}^{n}\left[f_{target}(i)\right]^2} \tag{6}$$

where n is the number of elements wherein the PDF is evaluated. The fitness value is set by the user as a calculation limit for the GA and Hybrid algorithms.

C. The Hybrid Algorithm

The third algorithm employed in this study is a hybrid of the single step and the GA algorithms. First, the single step algorithm is used to quickly determine the wanted subset of data. The resulting subset of data with moderate accuracy is then used to feed the iterative GA algorithm in the second step. The second step is used to accurately determine the final data subset. The GA hence has a smaller initial data set and a more accurate initial distribution of data, which leads to shorter computational times.

D. Accuracy of Sample-Selected Distributions

To quantify the error between the target- and final sample-selected PDFs, a mean sum-square error is defined as

$$\varepsilon_d = \frac{1}{n}\sum_{i=1}^{n}\left(f_{final}(i) - f_{target}(i)\right)^2 \Delta S_{21} \tag{7}$$

where n is the number of elements in the data vector and ΔS_{21} is the difference between two amplitude bins in the PDF. $f_{initial}(i)$ and $f_{final}(i)$ are the initial and final sample-selected PDFs, respectively. In addition to ε_d, the relative amount of remaining samples is noted, since it will affect the accuracy. Other error parameters were also considered. A dominating type of error is the statistical inaccuracy of the measurement, which is dependent of the number of independent samples, N_{ind}, in the initial distribution. When discarding some of the measured samples in a sequence, the measurement accuracy is affected, but not necessarily decreased. If the discarded samples do not contribute to the desired target distribution, the accuracy can actually be improved.

In order to see how the accuracy is affected by the sample selection technique, we choose to study the accuracy of the average power as a figure of merit for final target distribution accuracy. This is because MRSCs are often used to measure the antenna radiation efficiency, which is proportional to the average power of the measured sequence. In this contribution, the accuracy of average power is defined as the ratio between the standard deviation of the average power and the mean power. How the sample selection technique affects the accuracy can be studied by deriving and comparing this ratio before and after sample selection. For an exponentially distributed random variable, the standard deviation s and the mean value μ are equal. The central limit theorem states that the standard deviation is proportional to the inverse of the square root of the number of independent samples N_{ind} [34], whereas the mean remains the same. We thus find that the relative accuracy for the initial data (assumed to be Rayleigh-distributed) is

$$\varepsilon_{initial} = \frac{s_{initial}}{\mu_{initial}} \cdot \frac{1}{\sqrt{N_{ind,initial}}} = \frac{1}{\sqrt{N_{ind,initial}}} \tag{8}$$

where $N_{ind,initial}$ is the number of independent samples in the initial distribution. After having applied the sample-selection technique, the amplitude becomes Rician-distributed, with parameters a_{final} and s_{final}. The mean and standard deviation of the power of a single sample within a Rician-distributed set are given by

$$\mu_{final} = a_{final}^2 + 2s_{final}^2 \tag{9}$$

$$s_{final,2} = 2s_{final}^2\sqrt{1 + \frac{a_{final}^2}{s_{final}^2}} \tag{10}$$

This results in a relative accuracy of the final data of

$$\begin{aligned}\varepsilon_{final} &= \frac{s_{final,2}}{\mu_{final}} \cdot \frac{1}{\sqrt{N_{ind,final}}} \\ &= \frac{\sqrt{\frac{1+a_{final}^2}{s_{final}^2}}}{\frac{1+a_{final}^2}{\left(2s_{final}^2\right)}} \cdot \frac{1}{\sqrt{N_{ind,final}}},\end{aligned} \tag{11}$$

where $N_{ind,final}$ is the number of independent samples in the final distribution. From (11), we can see that after applying the sample-selection technique, an increased accuracy ($\epsilon_{initial} \geq \epsilon_{final}$) is possible in MSRCs. Determining the number of independent samples in the final subset ($N_{ind,final}$) represents a key issue. The number of independent samples of the original data set ($N_{ind,initial}$) is calculated by the techniques in [35], [36], wherein the oversampling ratio X is defined as

$$X = \frac{M_{initial}}{N_{ind,initial}} \tag{12}$$

where $M_{initial}$ is the number of measured samples in the initial set of data. When the algorithms are performing the sample selection process, independent samples are discarded every time a consecutive sequence of measured samples longer than or equal to the over sampling ratio is discarded. For example, in the case of $X = 3$, $N_{ind,initial}$ will not be reduced if 1–2 samples in a row are discarded. If 3–5 samples in a row are discarded, this reduces $N_{ind,initial}$ by one. If 6–8 samples in a row are discarded, this reduces $N_{ind,initial}$ by two, and so on. This means that in some cases $N_{ind,final}$ can be equal to $N_{ind,initial}$, but also that the accuracy of final subsets depends on the oversampling ratio of initial sample sets. This is why it was important to test the sample-selection technique over both simulated and measured initial data sets. In the worst case scenario, however, $N_{ind,initial}$ may be reduced by the same ratio as $M_{initial}$ (number of samples) when

$$1 \geq \frac{N_{ind,final}}{N_{ind,initial}} \geq \frac{M_{final}}{M_{initial}} \tag{13}$$

where M_{final} is the number of samples after the sample-selection algorithm (final subset). It is also important to notice that when going from a Rayleigh distribution to a Rician distribution, the first factor (s/μ) on the right-hand side of (11) will be lower in the final distribution than in the initial distribution, and this helps reducing the error of the technique. Therefore, the sample-selection technique is recommended to be used on rich multipath Rayleigh-fading initial data sets. This does not mean, however, that the technique does not work with other initial sets

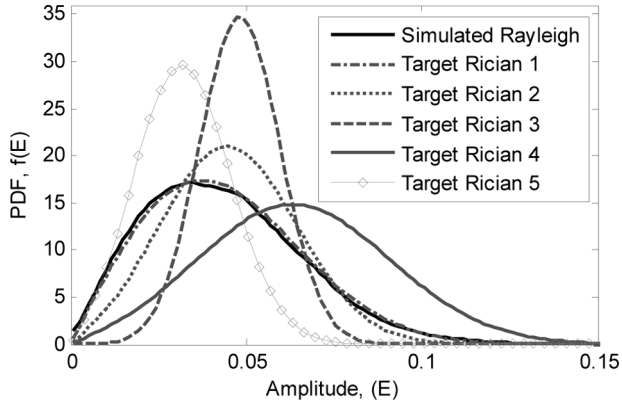

Fig. 1. Simulated Rayleigh and target (Rician) fading distributions. [15].

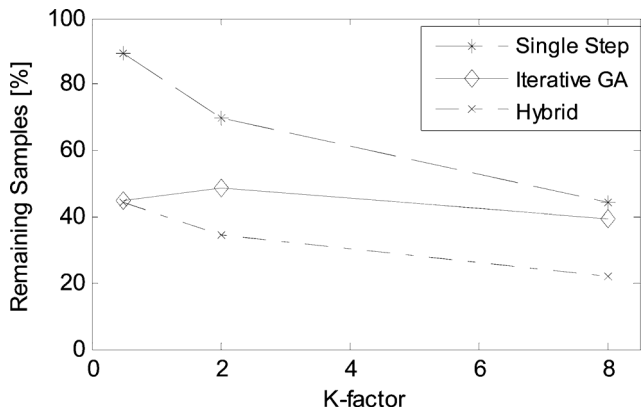

Fig. 2. Percentage of remaining samples for all algorithms versus K-factor.

TABLE I
THE FIVE DIFFERENT TARGET RICIAN DISTRIBUTIONS [15]

Target Distribution	a_{target}	s_{target}	*K-factor [linear]*	P_{out}/P_{in}
Rician 1	0.0286	0.0286	0.5	1
Rician 2	0.0404	0.0202	2	1
Rician 3	0.0467	0.0117	8	1
Rician 4	0.0572	0.0286	2	2
Rician 5	0.0286	0.0143	2	0.5

as the second factor in (11) typically increases the error, because $N_{ind,final} < N_{ind,initial}$.

III. SAMPLE SELECTION PERFORMANCE

A. Results Using Simulated Initial Data Sets

In this section the performance of the three different algorithms is analysed when a set of 10 000 simulated Rayleigh-distributed samples is used. The simulated data set is obtained by applying the $randn(M) + i \cdot randn(M)$ command in a Matlab™-script. Five different ideal Rician target distributions are defined in Fig. 1. The specific parameters for each distribution are also defined in Table I. Three of the distributions have the same mean power as the original distribution. Distributions 4 and 5 have higher and lower output power, respectively. The performance and errors of all algorithms with the previously-described simulated initial data are illustrated in Figs. 2–4.

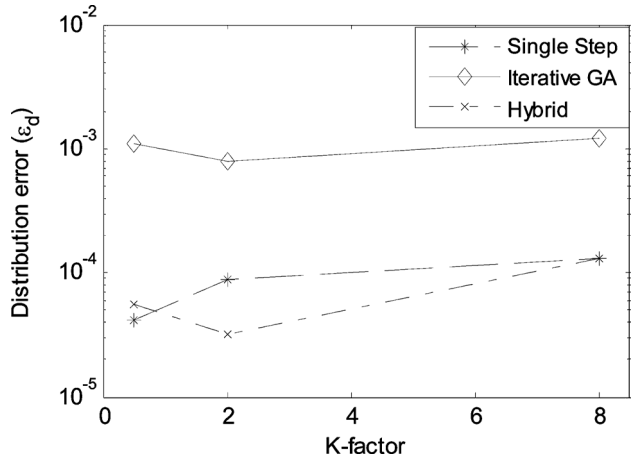

Fig. 3. Distribution error of all algorithms versus K-factor.

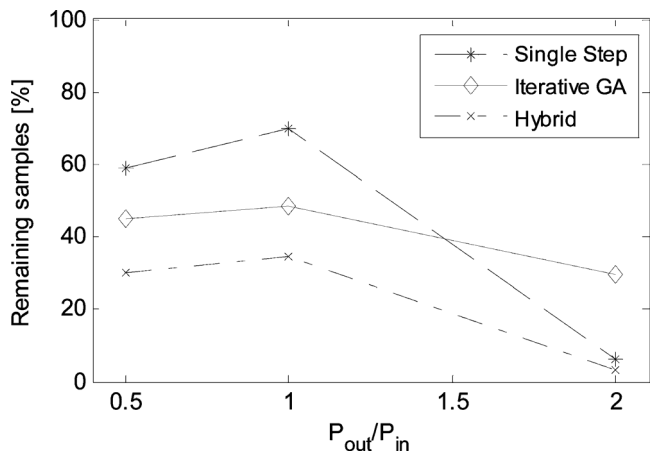

Fig. 4. The ratio Pout/Pin versus percentage of remaining samples for all algorithms. All distributions have the same $K = 2$ factor.

Fig. 2 depicts the evaluation of remaining samples due to changes in the target K factor for the same final output power than that in the initial data set (Rician targets 1, 2 and 3). In the results depicted in Fig. 2, the fitness limit of the iterative GA is set to 0.01 and the hybrid is set to 0.001. Fig. 3 illustrates the distribution error (ϵd) due to changes in the target K factor for the same final output power than that in the initial data set (Rician targets 1, 2 and 3). Fig. 4 depicts the amount of remaining samples due to changes in the ratio $P_{\rm out}/P_{\rm in}$ for the same final $K = 2$ factor (Rician targets 2, 4 and 5). It is worth mentioning here that the single-step algorithm is extremely fast and obtains all final subsets within a second, while the iterative GA and the hybrid algorithms took between 2 to 50 minutes and an average of 4.7 seconds, respectively.

B. Results Using Measured Initial Data Sets

This section shows how the sample selection technique performs with input data samples measured in MSRCs. In order to verify the performance of the technique with measured initial data sets, seven different MSRC-measured initial sample sets were employed, corresponding to emulated scenarios 'A' to 'G'. The measurements of the initial data sets were performed in the E200 MIMO Analyzer mode-stirred reverberation chamber.

TABLE II
THE DIFFERENT PAIRED TEST CASES

Test Case	1	2	3	4	5	6	7	8
Initial PDF	A	B	C	D	E	F	G	B
Target PDF	Meas on-body in MSRC							802.11n

The E200 was connected to a Rohde & Schwarz ZVRE Vector Network Analyzer. The E200 is an MSRC with dimensions of 0.82 m $\times$ 1.275 m $\times$ 1.95 m, eight exciting antennas, and polarization-stirring due to aperture-coupling and to the different orientation of the antenna exciting elements. An RMS DS of 90 ns was measured for the typical Rayleigh-fading test scenario. It also has three mechanical and mode-coupling stirrers, one holder-stirrer and a variable iris-coupling. E200 contains two cavities, the upper cavity with the transmitting antennas and the lower cavity wherein the receive MIMO antennas are placed. Coupling between upper and lower cavity is made through a slotted metal plate, and some control over the slotted apertures is achieved through the movements of stirrers. This provides a very rich Rayleigh-fading scenario within the lower cavity, when all measured samples and slots couplings are accounted for.

Scenario 'A' represents an empty MSRC, providing the typical Rayleigh-fading distribution. In scenarios 'B' to 'G' different pieces of absorbers are introduced inside the chamber in order to change the isotropic condition and the door is left open 60°. Since the dipoles do not receive the expected multipath component on the absorbed side, a non-isotropic scattering scenario is obtained with reduced multipath component (MPC) compared to the isotropic scenario 'A'. Details are provided in [18], [19].

Two different target PDFs were selected. The first target data was a measured one configured as an on-body channel with a real person in a large MSRC at Uppsala University. The MSRC at Uppsala University has a size of 4 m $\times$ 8 m $\times$ 2.3 m. In an effort to evaluate the validity of the sample selection technique to emulate amplitude PDFs of standardized channel models for compliance testing, the second selected target environment is a Matlab™-created standardized IEEE 802.11n channel model (MIMO-WLAN) [37], [38], which represents an accurate reproduction of a real IEEE 802.11n channel. The IEEE 802.11n target data sample set uses a 2 $\times$ 2 MIMO system at a frequency of 2.4 GHz with 9 propagation paths in an office environment. The seven different initial sample sets were paired together with the different target PDFs and named from 1 to 8, as illustrated in Table II.

After running all three sample-selection algorithms on all paired situations, analyses were performed considering the distribution error, remaining samples, power accuracy and number of independent samples, as described in Section II-D. All algorithms were run on a computer with Intel Pentium 4, Dual Core, 2.4 GHz and 740 Mbytes of RAM. The single step algorithm took a miniscule time, which averaged 0.6 s. The iterative GA took considerably longer computational times, ranging from 5 to 30 minutes, whereas the hybrid algorithm only took between 5 to 15 seconds. As running times depend on the selected fitness value (error limit as per (6)), Fig. 5 depicts a comparison

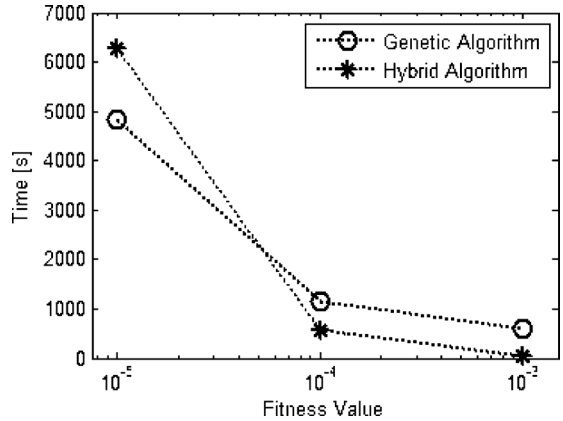

Fig. 5. Comparison of computational performance versus error limit for the iterative GA and hybrid algorithms for test case 8.

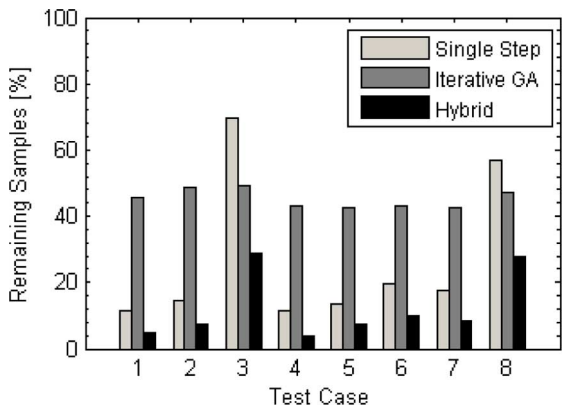

Fig. 6. Final percentage of remaining samples for all test cases.

of computational times versus fitness value for the GA and hybrid algorithms for test case 8. From this figure it seems clear that the hybrid algorithm outperforms the GA one for fitness values above 0.00005 (cross-over point). The percentage of remaining samples is illustrated in Fig. 6 for 0.001 fitness value. The GA always keep a larger percentage of remaining samples, as expected, but it is interesting to observe from this figure that the difference to those kept by the hybrid algorithm is not so large for case 8, when the target data set is the theoretical standardized IEEE 802.11n channel model. The results of analysed N_{ind} and the power accuracy (ε_{final}) are shown in Figs. 7 and 8, respectively. From Figs. 7 and 8 it is clearly observed that, despite a relatively large reduction in the total number of samples illustrated in Fig. 6, the number of independent samples is not proportionally reduced at all and the power accuracy is hardly affected by the sample-selection algorithms, with the only exception of case 4 for the step and hybrid algorithms. The best final power accuracy was that obtained when the initial data set was the measured scenario A (rich isotropic multipath). This will be discussed further on.

IV. MIMO ANTENNA PARAMETERS

To validate the results obtained with the sample selection technique, some final MIMO antenna parameters were estimated from the final sample-selected measured subsets. Three

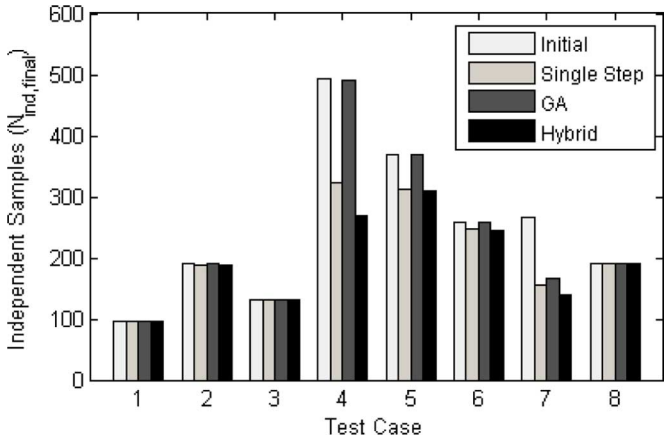

Fig. 7. Number of independent samples remaining in the final sample subsets compared with their initial set counterparts.

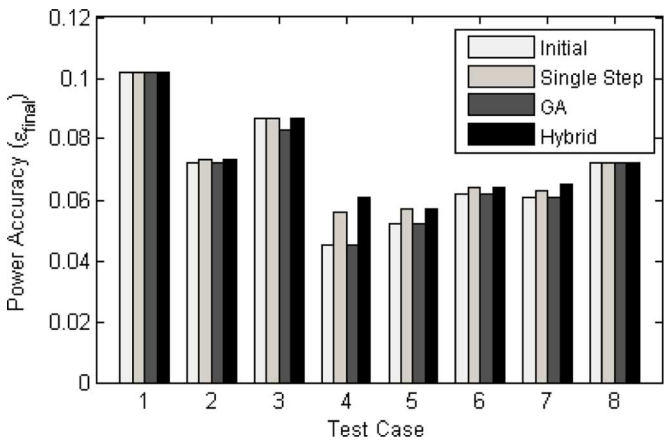

Fig. 8. Power accuracy for the final sample subsets compared with their initial set counterparts.

parallel dipoles ($f_c = 1800$ MHz,) in a vertical position and with a separating distance of $D = 0.05\lambda$ were employed as receive MIMO antennas in a 3×3 MIMO test system. Following the findings in the previous sections for getting accurate results, the initial data set was the measured sample set using scenario A at the E200 MIMO Analyzer (isotropic) with the three parallel dipoles as receive antennas. Three different Rician channels with different K-factors ($K = 0.01$, 4.26 and 49) were selected as target PDFs. The emulated results using the final sample-selected subsets were compared, in terms of MIMO capacity, with the theoretical upperbound model for Rician environments described in [36]. Results are illustrated in Fig. 9.

Since correlation between the antennas at the reception is high, the results were not expected to reach the maximum ergodic capabilities of the channel, as they are described in [38]. Yet, as the K-factor is increased, it was expected that correlation would play a less important role on MIMO capacity, i.e., the correlation has a strong influence in MIMO capacity as long as the K-factor is relatively low [39]. When the LoS path becomes the most important part of the signal, correlation has a much lower influence on the results of MIMO capacity [39]. The

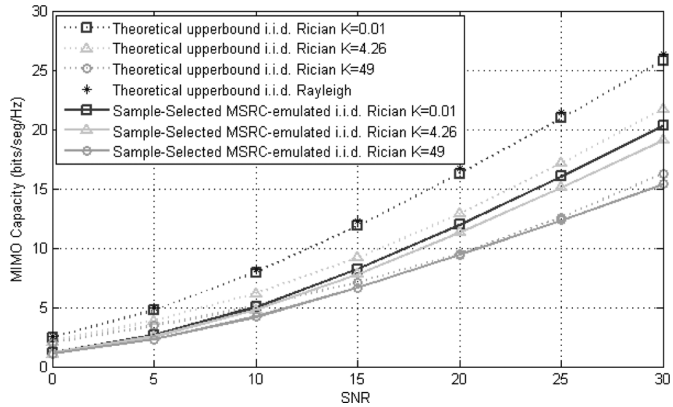

Fig. 9. 3×3 MIMO capacity emulated using the sample selection technique with different Rician K-factors.

results depicted in Fig. 9 clearly illustrate what was expected. MIMO Capacity differences between the sample-selected emulated channel and the theoretical upperbound i.i.d Rician results are high for low K-factor, decrease for moderate K factors and are nearly non-existent for high K-factors (49).

V. Discussion

Figs. 1–3 identify a clear constraint of the employed algorithms, and that is the fact that the target distribution should have the same mean power as the initial distribution for maintaining good accuracy in the final sample-selected results. The reason for this can be intuitively understood. If the output power is higher than the input power there will be a problem of finding data samples for the new distribution. This can also be observed from Fig. 5. Similarly, if lower power relative to the power of the initial distribution is targeted, the same problem occurs. Thus, the algorithm should only be used to achieve the correct K-factor and shape of distribution, and not as an amplifier or attenuator. Likewise, when the initial data set was that of measured scenario D in [18], [19], final sample-selected results suffered from a lack of accuracy and percentage of remaining samples in comparison to the results obtained when using other initial data sets. Since scenario D in [18], [19] represents the narrowest angular spread (AS), it is also easily understood that any sample-selected algorithm encounters difficulties extracting different PDFs from such extreme initial data. This, however, serves for suggesting that rich isotropic Rayleigh-fading initial data sets should be used for sample-selection techniques. This hypothesis is further confirmed with Figs. 4–6, wherein test case 1 (using rich multipath Rayleigh-fading isotropic scenario A as initial measured data set) outperforms any other initial data set.

It is worth mentioning that the technique is repeatable as long as the measured scenario does not change. Should the host PC (if used) change for a dongle RF-antenna front end prototype under test, o should the cylinder loading of the chamber change, results would be different and sample-selection procedures have to be run again. In this sense, once sample subsets have been selected for a specific measured scenario and antenna under test (AUT), these do not have to be changed for estimating different MIMO parameters.

VI. Conclusions

It has been demonstrated that the sample selection technique allows for the emulation of arbitrary amplitude PDFs using measured data in a mode-stirred reverberation chambers. This is demonstrated here for the first time. The technique neither requires any hardware alteration nor does it modify any measured sample at all. While the final emulated PDFs do not yet allow for changes in the fading physical parameters (PAS, AoA, etc.), it certainly represents a step forward towards arbitrary fading emulation using MSRCs.

The technique has also been validated for MIMO antenna parameters such as MIMO capacity. Among the identified limitations of the technique, it seems clear that the power of the final and initial data sets has to be the same, and that the use of initial rich multipath Rayleigh fading measured data sets provide better final subset accuracies. Three different algorithms have been successfully employed. The accuracy is adequate for most cases, but large differences in computational times have also been found. A trade-off between very accurate results with large percentage of remaining independent samples and speed is clearly observed. With the use of combined linear-GA, relatively accurate results can be obtained at low computational times, but there is certainly some room for improvement in this sense. The sample-selection technique can further enhance the capabilities of mode-stirred reverberation chambers for evaluating MIMO antenna parameters once amplitude-only channel models have been proposed for tier 1 standardized MIMO OTA testing. Future research includes the extension of the technique for active MIMO OTA tests as well as the development of enhancements in the technique for the emulation of a wide range of standardised channel models which include time-related properties such as delay spread and angular-related properties such as angular spread. The technique is patent protected by EMITE.

References

[1] "Measurements of Radio Performances for UMTS Terminals in Speech Mode," 2008, 3GPP TR 25.914 V7.0.0.

[2] T. Maeda and T. Morooka, "Radiation efficiency measurement method for electrically small antennas using radio wave scatterers," in *Proc. IEEE Antennas and Propagation Society Int. Symp.*, 1988, vol. 1, pp. 324–327.

[3] H. Arai and T. Urakawa, "Radiation power measurement using compact shield box," in *Proc. ISAP*, 1996, pp. 1005–1008.

[4] K. Madsén and P. Hallbjörner, "Reverberation chamber for mobile phone antenna tests," in *Reverberation Chamber, Anechoic Chamber and OATS Users Meeting*, Seattle, WA, Jun. 4–6, 2001.

[5] P. Corona, G. Latmiral, E. Paolini, and L. Piccioli, "Use of reverberating enclosure for measurements of radiated power in the microwave range," *IEEE Trans. Electromagn. Compat.*, vol. 18, no. 2, pp. 54–59, 1976.

[6] M. Lienard and P. Degauque, "Simulation of dual array multipath channels using mode-stirred reverberation chamber," *Electron. Lett.*, vol. 40, no. 10, pp. 578–579, May 2004.

[7] P. Corona, G. Ferrera, and M. Migliaccio, "Reverberating chambers as sources of stochastic electromagnetic fields," *IEEE Trans. Electromagn. Compat.*, vol. 38, no. 3, pp. 348–356, Mar. 1996.

[8] J. G. Kostas and B. Boverie, "Statistical model for a mode-stirred chamber," *IEEE Trans. Electromagn. Compat.*, vol. 33, no. 4, pp. 366–370, 1991.

[9] K. Rosengren, P. S. Kildal, C. Carlsson, and J. Carlsson, "Characterization of antennas for mobile and wireless terminals in reverberation chambers: Improved accuracy by platform stirring," *Microw. Opt. Technol. Lett.*, vol. 30, no. 20, pp. 391–397, Sep. 2001.

[10] K. Rosengren and P. S. Kildal, "Radiation efficiency, correlation, diversity gain, and capacity of a six monopole antenna array for a MIMO system: Theory, simulation and measurement in reverberation chamber," *Proc. IEE: Microw., Antennas, Propag.*, vol. 152, no. 1, pp. 7–16, Feb. 2005.

[11] M. Otterskog and K. Madsen, "On creating a nonisotropic propagation environment inside a scattered field chamber," *Microw. Opt. Technol. Lett.*, vol. 43, no. 3, pp. 192–195, Nov. 2004.

[12] K. A. Remley, S. J. Floris, H. A. Shah, and C. L. Holloway, "Static and dynamic propagation-channel impairments in reverberation chambers," *IEEE Trans. Electromagn. Compat.*, vol. 53, no. 3, pp. 589–599, 2011.

[13] T. A. Loughry and S. H. Gurbaxani, "The effects of intrinsic test fixture isolation on material shielding effectiveness measurements using nested mode-stirred chambers," *IEEE Trans. Electromagn. Compat.*, vol. 37, no. 3, pp. 449–452, Mar. 1995.

[14] Z. Yun and M. F. Iskander, "MIMO capacity for realistic wireless communications environments," in *Proc. IEEE Antennas Propag. Soc. Int. Symp.*, Jun. 2004, pp. 1231–1234.

[15] H. Arai, "Field simulator for Rayleigh/Rician fading reproduction," in *Proc. IEEE Antennas Propag. Soc. Int. Symp.*, 1996, vol. 2, pp. 1218–1221.

[16] P. Hallbjörner, "Reverberation chamber with variable field amplitude distribution," *Microw. Opt. Technol. Lett.*, vol. 35, no. 5, pp. 376–377, 2002.

[17] H. Fielitz, K. A. Remley, C. L. Holloway, Q. Zhang, Q. Wu, and D. W. Matolak, "Reverberation chamber test environment for outdoor urban wireless propagation studies," *IEEE Antennas Wireless Propag. Lett.*, vol. 9, pp. 52–56, 2010.

[18] J. F. Valenzuela-Valdes, A. M. Martinez-Gonzalez, and D. A. Sanchez-Hernandez, "Emulation of MIMO nonisotropic fading environments with reverberation chambers," *IEEE Antennas Wireless Propag. Lett.*, vol. 7, pp. 325–328, 2008.

[19] J. F. Valenzuela-Valdes, A. M. Martinez-Gonzalez, and D. A. Sanchez-Hernandez, "Diversity gain and MIMO capacity for nonisotropic environments using a reverberation chamber," *IEEE Antennas Wireless Propag. Lett.*, vol. 8, pp. 112–115, 2009.

[20] C. L. Holloway, D. A. Hill, J. M. Ladbury, P. F. Wilson, G. Koepke, and J. Coder, "On the use of reverberation chambers to simulate a Rician radio environment for the testing of wireless devices," *IEEE Trans. Antennas Propag.*, vol. 54, no. 11, pp. 3167–3177, Nov. 2006.

[21] D. M. Zhang, E. P. Li, T. K. D. Yeo, W. S. Chow, and J. Quek, "Influences of loading absorber on the performances of a reverberation chamber," in *Proc. Int. Symp. Electromagn. Compat.*, 2003, vol. 1, pp. 279–281.

[22] J. D. Sánchez-Heredia, J. F. Valenzuela-Valdés, A. M. Martinez-González, and D. A. Sánchez-Hernández, "Emulation of MIMO Rician-fading environments with mode-stirred reverberation chambers," *IEEE Trans. Antennas Propag.*, vol. 59, no. 2, pp. 654–660, Feb. 2011.

[23] A. Cozza and A. E. A. el-Aileh, "Accurate radiation-pattern measurements in a time-reversal electromagnetic chamber," *IEEE Antennas Propag. Mag.*, vol. 52, no. 2, pp. 186–193, 2010.

[24] R. J. Pirkl (NIST) and K. A. Remley (NIST), "Multipath angle-of-Arrival in reverberation chambers,," in *Program Working Group Contribution Document MOSG110304*, 2011.

[25] A. Sorrentino, G. Ferrara, and M. Migliaccio, "The reverberating chamber as a line-of-sight wireless channel emulator," *IEEE Trans. Antennas Propag.*, vol. 56, no. 6, pp. 1825–1830, Jun. 2008.

[26] M. A. García-Fernández, J. D. Sánchez-Heredia, A. M. Martínez-González, D. A. Sánchez-Hernández, and J. F. Valenzuela-Valdés, "Advances in mode-stirred reverberation chambers for wireless communication performance evaluation," *IEEE Commun. Mag.*, pp. 140–147, Jul. 2011.

[27] J. D. Sánchez-Heredia, M. Grudén, J. Valenzuela-Valdés, and D. A. Sánchez-Hernández, "Sample selection method for Rician-fading emulation using mode-stirred chambers," *IEEE Antennas Wireless Propag. Lett.*, vol. 9, pp. 409–412, 2010.

[28] S. P. Prather (AT&T) and A. Youtz (Verizon Wireless), "OTA performance criteria for MIMO devices," in *CTIA Certification Program Working Group Contribution Document MOSG110707*, Jul. 2011.

[29] Elektrobit, "Verified performance: Anechoic chamber and fading emulator based MIMO OTA," in *TSG-RAN WG4 Meeting AH#4 Document R4-103856*, Xi'an, China, Oct. 2010.

[30] A. D. Panagopoulos, K. P. Liolis, and P. G. Cottis, "Rician K-factor distribution in broadband fixed wireless access channels under rain fades," *IEEE Commun. Lett.*, vol. 11, no. 4, pp. 301–303, 2007.

[31] X. Hu, Y. Zhang, Y. Jia, S. Zhou, and L. Xiao, "Power coverage and fading characteristics of distributed antenna systems," in *Proc. 4th Int. Conf. Commun. Netw. China (ChinaCOM)*, 2009, pp. 1–4.
[32] S. Guatelli, B. Mascialino, A. Pfeiffer, M. G. Pia, A. Ribon, and P. Viarengo, "Application of statistical methods for the comparison of data distributions," in *Proc. IEEE Nucl. Sci. Symp. Conf. Rec.*, 2004, vol. 4, pp. 2086–2090.
[33] R. O. Duda, P. E. Hart, and D. G. Stork, *Pattern Classification*, 2nd ed. New York: Wiley, 2001.
[34] L. Råde and B. Westergren, *Mathematics Handbook for Science and Engineering*. Germany: Studentlitteratur AB, 2003.
[35] P. Hallbjörner, "A model for the number of independent samples in reverberation chambers," *Microw. Opt. Technol. Lett.*, vol. 33, no. 1, pp. 25–28, 2002.
[36] P. Hallbjörner, "Estimating the number of independent samples in reverberation chamber measurements from sample differences," *IEEE Trans. Electromagn. Compat.*, vol. 48, no. 2, pp. 354–358, 2006.
[37] J. P. Kermoal, L. Schumacher, K. I. Pedersen, P. E. Morgensen, and F. Frederiksen, "A stochastic MIMO radio channel model with experimental validation," *IEEE J. Sel. Areas Commun.*, vol. 20, no. 6, pp. 1211–1226, 2002.
[38] V. Erceg, TGn Channel Models 2004, IEEE 802.11 document 03/940r4.
[39] M. Kang and M. S. Alouini, "Capacity of MIMO Rician channels," *IEEE Trans. Wireless Communications*, vol. 5, pp. 112–122, 2006.

Adoración Marín-Soler was born in Ceutí, Spain. She received the Technical Telecommunication Engineering degree the Telecommunication Engineering degree from the Universidad Politécnica de Cartagena, Spain, in 2008 and 2010, respectively, where she is currently pursuing the Ph.D. degree in the Department of Information Technologies and Communications.

In 2009, she had a short stay at Loughborough University working on microwave focusing planar antennas for medical applications. In 2011 she joined EMITE. Her current research areas cover antennas, MIMO communications and mode-stirred reverberation chambers.

Mathias Grudén was born in 1985, in Mora, Sweden. He received the M.Sc. degree in engineering physics from Uppsala University, Sweden, in 2009, where he is currently pursuing the Ph.D. degree in the group of Applied Microwave and Millimeterwave Technology.

The main areas of the current research are antenna measurement techniques and communication for wireless sensor networks in electromagnetic harsh environment such as onboard train wagons and inside aircraft jet engines.

Juan D. Sánchez-Heredia was born in Lorca, Spain. He received the Telecommunication Engineering Degree from the Universidad Politécnica de Cartagena, Spain, in 2009 which culminated with the Final Degree Award. In 2010 he received the M.Sc. degree in information technology (IT) from Universidad de Murcia, Spain. In 2009, he joined the Department of Information Technologies and Communications, Universidad Politécnica de Cartagena, where he is currently pursuing the Ph.D. degree.

In 2007 he worked at General Electric, Cartagena, and was involved in several projects in relation with the network infrastructure. His current research areas cover MIMO communications, multimode-stirred chambers and electromagnetic dosimetry.

Paul Hallbjörner was born in Uppsala, Sweden, in 1966. He received the B.Sc. degree in 1988, the M.Sc. degree in 1995, and the Ph.D. degree in 2005, all in electrical engineering, from Chalmers University of Technology, Göteborg, Sweden.

He has worked in the telecom industry since 1989, mainly with antennas and microwave technology. Since 2000, he has been working as an antenna researcher, with main focus on antenna design and measurement methods for mobile phone systems and short range communication. Apart from this, he has worked with reconfigurable and steerable antennas, wave propagation, passive microwave circuits, material characterization, and millimeter-wave building practice. He has been employed by Ericsson, Saab, Allgon, and is currently with SP Technical Research Institute of Sweden. He has more than 60 scientific publications and is the inventor to nine patents.

Antonio M. Martínez-González received the Dipl.-Ing. in telecommunications engineering from Universidad Politécnica de Valencia, Spain, in 1998 and the Ph.D. degree from Universidad Politécnica de Cartagena,Spain, in early 2004.

From 1998 till September 1999, he was employed as Technical Engineer at the Electromagnetic Compatibility Laboratory of Universidad Politécnica de Valencia, where he developed assessment activities and compliance certifications with European directives related with immunity and emissions to electromagnetic radiation from diverse electrical, electronic and telecommunication equipment. Since September 1999 he has been an Associate Professor at Universidad Politécnica de Cartagena. At present, his research interest is focused on electromagnetic dosimetry, radioelectric emissions and mode stirred chambers applied to MIMO systems. In December 2006 Dr. Martínez-González is one of the founders of EMITE, a technological spin-out company founded by Telecommunication Engineers and Doctors of the Microwave, Radiocommunications and Electromagnetism Research Group (GIMRE) of the Technical University of Cartagena , Spain.

Dr. Martínez-González's founding of EMITE took place right after the second i-patentes prize to innovation and technology transfer in the Region of Murcia Spain was awarded to the company founders. In 2008 GIMRE group was awarded this prize again.H is research works were awarded with the Spanish National Prize from Foundation Airtel and Colegio Oficial de Ingenieros de Telecomunicación de España to the best final project on Mobile Communications in 1999.

Anders Rydberg (M'89) received the M.Sc. degree from Lund Institute of Technology, Lund, Sweden, in 1976. In 1988 he received the Ph.D. degree from Chalmers University of Technology, Sweden.

In 1991, he was appointed Docent (Associated Professor) at Chalmers University. He worked between 1977–1983 at the National Defence Research Establishment, ELLEMTEL Development Co., and the Onsala Space Observatory. Between 1990 and 1991, he worked as a Senior Research Engineer at Farran Technology Ltd., Ireland. In 1992 he was employed as Associated Professor and in 2001 as Professor in Applied Microwave and Millimeterwave Technology at Uppsala University, Sweden. He is heading the Microwave Group at the Department of Engineering Science, Uppsala University. Since 2007, he has also been also joint-owner of Integrated Antennas AB, Uppsala, Sweden. He has authored or co-authored more than 190 publications in the area of micro- and millimeterwave antennas, sensors, solid state components and circuits and has three patents in the areas.

Prof. Rydberg is a member of the editorial board for the IEEE-MTT, adjunct member of Sections B and D of the Swedish Member Committee of URSI (SNRV) and Chairman for the Swedish IEEE MTT/AP Chapter

David A. Sánchez-Hernández (M'00–SM'06) received the Dipl.-Ing. in telecommunications engineering from Universidad Politécnica de Valencia, Spain, in 1992 and the Ph.D. degree from King's College, University of London, in 1996.

From 1992 to 1994, he was employed as a Research Associate for The British Council-CAM at King's College London where he worked on active and dual-band microstrip patch antennas. In 1994 he was appointed EU Research Fellow at King's College London, working on several joint projects at 18, 38 and 60 GHz related to printed and integrated antennas on GaAs, microstrip antenna arrays, sectorization and diversity. In 1997 he returned to Universidad Politécnica de Valencia, Spain, where was co-leader of the Antennas, Microwaves and Radar Research Group and the Microwave Heating Group. In early 1999 he received the Readership from Universidad Politécnica de Cartagena, and was appointed Vice Dean of the School for Telecommunications Engineering and leader of the Microwave, Radiocommunications and Electromagnetism Engineering Research Group. In late 1999 he was appointed ViceChancellor for Innovation and Technology Transfer at Universidad Politécnica de Cartagena and member of several Foundations and Societies for promotion of R&D in the Autonomous Region of Murcia, in Spain. In May 2001, he was appointed official advisor in technology transfer and member of The Industrial Advisory Council of the Autonomous Government of the Region of Murcia, in Spain, and in May 2003 he was appointed Head of Department. He obtained the Signal Theory and Communications Chair in 2009. He has published over 50 scientific papers and over 100 conference contributions, and is a reviewer of several international journals. He holds five patents. His current research interests encompass all aspects of the design and application of printed multi-band antennas for mobile communications, electromagnetic dosimetry issues and MIMO techniques for wireless communications.

Prof. Sánchez-Hernández is a Chartered Engineer (CEng), IET Fellow, CENELEC TC106X member, and is the recipient of the R&D J. Langham Thompson Premium, awarded by the Institution of Electrical Engineers (now formerly the Institution of Engineering and Technology), as well as other national and international awards. He is the co-founder of EMITE Ing.